

Groundwater Storage Change in the Jinsha River Basin from GRACE, Hydrologic Models, and In Situ Data

by Nengfang Chao^{1,2}, Gang Chen¹, Jian Li¹, Longwei Xiang^{3,4}, Zhengtao Wang^{5,6}, and Kunjun Tian^{5,6}

Abstract

Groundwater plays a major role in the hydrological processes driven by climate change and human activities, particularly in upper mountainous basins. The Jinsha River Basin (JRB) is the uppermost region of the Yangtze River and the largest hydropower production region in China. With the construction of artificial cascade reservoirs increasing in this region, the annual and seasonal flows are changing and affecting the water cycles. Here, we first infer the groundwater storage changes (GWSC), accounting for sediment transport in JRB, by combining the Gravity Recovery and Climate Experiment mission, hydrologic models and in situ data. The results indicate: (1) the average estimation of the GWSC trend, accounting for sediment transport in JRB, is 0.76 ± 0.10 cm/year during the period 2003 to 2015, and the contribution of sediment transport accounts for 15%; (2) precipitation (P), evapotranspiration (ET), soil moisture change, GWSC, and land water storage changes (LWSC) show clear seasonal cycles; the interannual trends of LWSC and GWSC increase, but P , runoff (R), surface water storage change and SMC decrease, and ET remains basically unchanged; (3) the main contributor to the increase in LWSC in JRB is GWSC, and the increased GWSC may be dominated by human activities, such as cascade damming and climate variations (such as snow and glacier melt due to increased temperatures). This study can provide valuable information regarding JRB in China for understanding GWSC patterns and exploring their implications for regional water management.

Introduction

Groundwater is the foremost freshwater resource and plays a critical role in the global water cycle (Seiler and Gat 2007; Margat and van de Gun 2013). Due to

global climate change and the increasing population, the groundwater storage in some regions is decreasing, but in other places it is increasing (Hanjra and Qureshi 2010). It is important to understand the changes in groundwater at global and regional scales (Oki and Kanae 2006; Schlosser et al. 2014).

Due to lack of investment, and the cost and difficulty associated with drilling monitoring wells, groundwater depth measurements in wells have been more difficult than for surface water. The seasonal recharges from precipitation and runoff are complex and fluctuate, making the temporal assessment of groundwater more challenging (Ireson et al. 2006; Gleeson et al. 2016; Chang et al. 2017). It is critical for water management to understand the spatiotemporal variability of groundwater storage (Alley et al. 2002, 2018).

Techniques such as remote sensing provide a unique way to investigate hydrological processes, and research has shown that monitoring water resources from satellite observation data is reliable (Alsdorf et al. 2007; Rast et al. 2014). In particular, the Gravity Recovery and Climate Experiment (GRACE) mission, launched in 2002, detected the time-variable gravity field, which can be inverted to the spatiotemporal variability of the land water storage changes (LWSC) at monthly or submonthly time scales (Tapley et al. 2004). LWSC include changes in

¹Corresponding author: College of Marine Science and Technology, China University of Geosciences, 388 Lu Mo Road, Wuhan, 430074, People's Republic of China. chaonf@cug.edu.cn

²Hubei Subsurface Multi-scale Imaging Key Laboratory, Institute of Geophysics and Geomatics, China University of Geosciences, 388 Lu Mo Road, Wuhan, 430074, People's Republic of China.

³State Key Laboratory of Geodesy and Earth's Dynamics, Institute of Geodesy and Geophysics, Chinese Academy of Sciences, 340 Xu Dong Street, Wuhan, 430077, People's Republic of China.

⁴University of Chinese Academy of Sciences, No.19(A) Yuquan Road, Shijingshan District, Beijing 100049, People's Republic of China.

⁵School of Geodesy and Geomatics, Wuhan University, 129 Luo Yu Road, Wuhan, 430079, People's Republic of China.

⁶Collaborative Innovation Center of Geospatial Technology, Wuhan University, 129 Luo Yu Road, Wuhan, 430079, People's Republic of China.

Article impact statement: Changes in groundwater storage when accounting for sediment transport in the Jinsha River Basin are increasing.

Received May 2019, accepted November 2019.

© 2019, National Ground Water Association.

doi: 10.1111/gwat.12966

snow/glaciers, surface water, soil moisture, and groundwater. Therefore, groundwater storage changes (GWSC) can be separated from LWSC measures by combining the GRACE data and external information (see Frappart and Ramillien [2018] and Feng et al. [2018] for a review on the use of GRACE for monitoring GWSC). The GRACE mission has proven to be a valuable tool for detecting GWSC at global (Richey et al. 2015; Rodell et al. 2018) and regional scales ($\sim 160,000 \text{ km}^2$) (Rodell et al. 2009a, 2009b; Voss et al. 2013; Chao et al. 2018).

Although there has been plenty of research using GRACE to explore GWSC in various river basins around the world, including the Amazon River Basin (South America) (Frappart et al. 2019), Tigris-Euphrates Basin (Middle East) (Chao et al. 2018), Congo Basin (Africa) (Ndehedehe et al. 2018), Canning Basin (Australia) (Munier et al. 2012), Colorado River Basin (USA) (Castle et al. 2014), Mississippi River basin (USA) (Rodell et al. 2007), and Yellow River Basin (China) (Lin et al. 2019), there has seldom been any thorough assessment of GWSC in the Jinsha River Basin (JRB), which is located in the uppermost region of the Yangtze River, China.

JRB ($24^{\circ}23'$ to $35^{\circ}46'N$, $90^{\circ}23'$ to $104^{\circ}37'E$) is one of the most important sediment sources for the Yangtze River and is the largest hydropower production region in China. The source of JRB is the Qinghai-Tibet Plateau (QTP), which is widely known as the “Third Pole” and the “Water Tower of Asia”. JRB includes the Jinsha River and its largest tributary the Yalong River, and covers four provinces (Qinghai, Xizang, Yunnan, and Sichuan) in China, with an area of approximately $500,000 \text{ km}^2$, accounting for 27.8% of the Yangtze River Basin. Human activities including damming and forest planning have been conducted in this region. Four large reservoirs [Wudongde (WDD), Baihetan (BHT), Xiluodu (XLD), and Xiangjiaba (XJB)] in the lower Jinsha River and eight reservoirs in the middle Jinsha River will be or have been constructed in recent years (Figure 1, Table 1). The installed hydropower generation capacity of WDD, BHT, XLD, and XJB combined is $4.0 \times 10^9 \text{ kW}$, which is twice the capacity of the Three Gorges Reservoir (TGR). Their total storage capacity is $4.1 \times 10^9 \text{ m}^3$, which is larger than TGR's at $3.9 \times 10^9 \text{ m}^3$. These cascaded reservoirs will further change the annual and seasonal flows and sediment regimes, and will affect water cycles. With increasing disturbances from dams, there is an urgent need to draw attention to the effects of the construction of cascading hydropower stations on riverine hydrologic cycles.

The purpose of this study is to obtain the GWSC accounting for sediment mass change in JRB between 2003 and 2015, by decomposing LWSC from the GRACE mission into the individual contributions of other hydrological components [such as soil moisture change (SMC), surface water storage change (SWSC), and GWSC] from satellite data, hydrologic models and in situ data.

The main contributions and novelties of this study are as follows: (1) the accuracy of precipitation (P) and

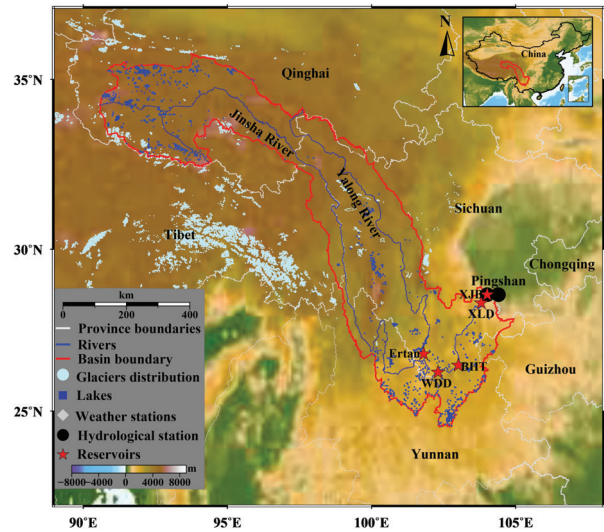


Figure 1. The location of JRB and its distribution of hydrometeorological stations, lakes, glaciers, and main artificial reservoirs.

evapotranspiration (ET) from different source data are first assessed by comparing them with the in situ data; (2) LWSC are inferred from different GRACE products, and are verified by in situ data of P , ET, and runoff (R) to determine the best one; (3) the GWSC accounting for sediment mass change in JRB between 2003 and 2015 are first derived; (4) the P , ET, SMC, SWSC, LWSC, GWSC, human-induced GWSC (HWGSC), and their seasonal and trend and interannual will be investigated.

Datasets and Methods

Datasets

GRACE Data

This study used three open source GRACE Mascons solutions, namely, Jet Propulsion Laboratory Mascons, Center for Space Research Mascons and Goddard Space Flight Center Mascons, in order to obtain LWSC. LWSC are also obtained from (<http://grace.jpl.nasa.gov/data/gracemonthlymassgridsland/>) by using the scale factor (SF) method (Landerer and Swenson 2012). The processing method is the same as that used in Rodell et al. (2018). That is, the degree-2 harmonic coefficients in the three solutions were replaced by those from satellite laser ranging solutions (Cheng et al. 2011), and the degree-one coefficients were from Swenson et al. (2008). All three solutions were corrected for the effect of glacial isostatic adjustment using the ICE-6G_D model (Peltier et al. 2015, 2017).

Hydrologic Model

1. GLDAS: The Global Land Data Assimilation System (Rodell et al. 2004) produces optimal fields of land surface states and fluxes in near-real time by combining satellite and ground-based observations into

Table 1
Basic Information about Some Cascaded Reservoirs in JRB (Modified from Li et al. 2018)

Reservoirs	Operation Time	Storage Capacity (10^8 m^3)	Watershed Area (10^4 km^2)	Installed Capacity (10^4 kW)	Location
Ertan (ET)	1999	58	11.64	330	Yalong River
Jinanjiao (JAQ)	2010.10	9.13	23.74	240	Middle Jinsha River
Ahai (AH)	2011.12	8.06	23.54	200	Middle Jinsha River
Jinping-2 (JP-2)	2012	0.14	10.3	480	Yalong River
Guandi (GD)	2012	7.6	11	240	Yalong River
Xiangjiaba (XJB)	2012.10	115.7	45.9	640	Lower Jinsha River
Longkaikou (LKK)	2012.11	5.58	24	180	Middle Jinsha River
Jinping-1 (JP-1)	2013	77.6	10.26	360	Yalong River
Ludila (LDL)	2013.4	17.18	24.73	216	Middle Jinsha River
Xiluodu (XLD)	2013.5	126.7	45.4	1386	Lower Jinsha River
Tongzilin (TZL)	2014	0.91	12.85	60	Yalong River
Guanyinyan (GY)	2014.10	0.72	25.65	300	Middle Jinsha River
Liyuan (LY)	2014.11	7.27	22	240	Middle Jinsha River
Longpan (LP)	*	371	21.4	420	Middle Jinsha River
Liangjiaren (LJR)	*	74.2	21.84	320	Middle Jinsha River
Wudongde (WDD)	*	74	40.61	870	Lower Jinsha River
Baihetan (BHT)	*	206	43.03	1350	Lower Jinsha River

Note: “*” indicates that the dam is under construction. The bold reservoirs (WDD, BHT, XLD, and XJB) are the four large hydropower stations in JRB.

four land surface models: the Community Land Model (CLM), the Mosaic (MOS) model, the Variable Infiltration Capacity (VIC) model, and the National Centers for Environmental Prediction/Oregon State University/Air Force/Hydrologic Research Lab Model (NOAH). Surface water storage in lakes, reservoirs, and river channels is not included in the GLDAS modeling system (Rodell et al. 2004). Here, surface water is from in situ runoff data (Thomas and Famiglietti 2019). Although the surface water’s contribution is usually small for most river basins and it is sometimes simply ignored, here, the GWSC is obtained by GRACE subtracting the GLDAS, surface water, and sediment mass change. Details can be seen in Section 2.2.2.

2. CLM4.0: The simulation data of soil moisture, snow, vegetation canopy storage, water storage in rivers, and groundwater (2003 to 2015) from the National Center for Atmospheric Research CLM4.0 (Bonan et al. 2011) are used in this study. Here, CLM4.0 is combined with GRACE data to infer the HGWSC. Moreover, CLM4.0 and GLDAS are used to determine the uncertainty in LWSC (Forootan et al. 2014).

P, ET, and R from Different Products

1. Precipitation (*P*): It is obtained from the level-3 monthly data of the Tropical Rainfall Measuring Mission (TRMM, 3B43 version 7) with a spatial resolution of $0.25 \times 0.25^\circ$ (Huffman et al. 2007), from the Global Precipitation Climatology Project (GPCP) (Adler et al. 2003) with a $1^\circ \times 1^\circ$ grid over the entire globe at 1-day (daily) intervals, from the four-monthly land surface model simulations (CLM, MOS, VIC, and NOAH) with the monthly and spatial resolution of a $1^\circ \times 1^\circ$ grid from GLDAS (Rodell et al. 2004), and from China Ground

Climate Daily Observation Data (CGCD) (<http://data.cma.cn>) with meteorological stations distributed across JRB (Figure 1).

2. Evapotranspiration (ET): It is from different products, that is, monthly ET products from four GLDAS models, Moderate Resolution Imaging Spectroradiometer (MODIS) (Mu et al. 2007) and CGCD.

3. Runoff (*R*): Runoff data from Pingshan and XJB are used to infer LWSC across JRB by using the water balance closure. *R* is the total runoff change over JRB, which is the difference between inflow and outflow. Please note that the hydrological control station in JRB is Pingshan before 2012 and XJB after 2012.

Climate Variability Indices

According to the research of Hasanean (2004) and Forootan et al. (2016), the Niño-3.4 for the El Niño–Southern Oscillation (ENSO) index (Rayner et al. 2003), Mediterranean Oscillation Index (MOI) (Martin-Vide and Lopez-Bustins 2006), and North Atlantic Oscillation (NAO) index (Rogers 1984) might have significant influences on the regional scale climate and water storage changes. Therefore, the Niño-3.4, MOI and NAO index will be used to study the climate change effects on the hydrologic variables in JRB.

The detailed information of the datasets and usages can be seen in Table 2.

Methods

Verification of P, ET, and LWSC

The precipitation from TRMM, GPCP, and the four GLDAS models (NOAH, VIC, CLM, and MOS), and ET from MODIS and the four GLDAS models are compared

Table 2
Summary of Datasets Used in This Study

Products	Data	Time	References	Sources
Land water storage change (LWSC)	GRACE	2002 to 2015	Landerer and Swenson 2012; Wiese et al. 2016; Save et al. 2016; Luthcke et al. 2013	Satellite remote sensing
Precipitation (P)	CLM4.0	2003 to 2015	Bonan et al. 2011	Satellite remote sensing
	TRMM-3B43	2003 to 2013	Huffman et al. 2007	Satellite remote sensing
	GPCP	2003 to 2013	Adler et al. 2003	Satellite remote sensing
	GLDAS (CLM), MOS model, VIC model, and National Centers for Environmental Prediction/Oregon State University/Air Force/Hydrologic Research Lab Model (NOAH)	2003 to 2015	Rodell et al. 2004	Satellite remote sensing
	CGCD observation data	2003 to 2013	http://data.cma.cn/site/index.html	In situ
Evapotranspiration (ET)	MODIS	2003 to 2013	Mu et al. 2007	Satellite remote sensing
	GLDAS (CLM, MOS, VIC, and NOAH)	2003 to 2015	Rodell et al. 2004	Satellite remote sensing
	CGCD observation data	2003 to 2013	http://data.cma.cn/site/index.html	In situ
Runoff (R), SWSC, and Sediment change (SC)	Chang Jiang Water Resources Commission of the Ministry of Water Resources in China	1995 to 2017	http://www.cjw.gov.cn/	Pingshan and XJB
Climate Indices	Niño-3.4, MOI, and NAO	1995 to 2017	https://www.esrl.noaa.gov/psd/data/climateindices/list/	
SMC	GLDAS	2003 to 2015	Rodell et al. 2004	Satellite remote sensing
Groundwater storage change (GWSC)	GRACE-GLDAS-Surface-Sediment	2003 to 2015		
HGWSC	GRACE-CLM4.0	2003 to 2015		

with in situ data. To verify LWSC, the time derivative (dS/dt) is determined (Famiglietti et al. 2011; Long et al. 2014) by the following equations:

$$dS/dt = P - ET - R \quad (1)$$

$$\frac{dS}{dt} \approx \frac{dLWSC}{dt} \approx \frac{LWSC(t) - LWSC(t-1)}{\Delta t} \quad (2)$$

Since dS/dt estimated from GRACE via the central difference scheme in Equation 2 above approximates the “true” derivatives, and in order to be temporally consistent with LWSC from GRACE data, Swenson and Wahr (2006) proposed to smooth the time series of the other water cycle variables according to

$$\tilde{F}_t = \frac{1}{4}F_{t-1} + \frac{1}{2}F_t + \frac{1}{4}F_{t+1} \quad (3)$$

where the F variables are time series of P , ET , and R . The indices $t-1$, t , and $t+1$ refer to the previous, current, and following month, respectively.

The following indicators are used to evaluate the precision of P , ET , and $LWSC$:

(1) The root mean square error (RMSE) determines model correctness:

$$RMSE = \left(\frac{1}{N_v} \sum_{i=1}^{N_v} (y_i - o_i)^2 \right)^{1/2} \quad (4)$$

where y_i and o_i are model (LWSC) and in situ values, respectively, and N_v is the number of target data values used for testing; (2) the RMSE scale where R^* ($=RMSE/\sigma_0$) is the ratio of the RMSE to the standard deviation of the observational value σ_0 , and is not smaller than zero; (3) the correlation coefficient; (4) the maximum absolute error ($MAE = \frac{1}{N_v} \sum_{i=1}^{N_v} |y_i - o_i|$) (Sun 2013; Long et al. 2014); (5) the Nash–Sutcliffe

efficiency ($NSE = 1 - \frac{\sum_{i=1}^{N_v} (y_i - o_i)^2}{\sum_{i=1}^{N_v} (o_i - \bar{o})^2}$) lies within the range

of $(-\infty, 1)$ and reflects the relationship between the forecasted and average observational values (Sun 2013; Long et al. 2014). Based on the different models, the very good, good, and satisfactory performances are defined as $NSE > 0.75$ and $R^* < 0.60$; $NSE > 0.65$ and $R^* < 0.60$; and $NSE > 0.5$ and $R^* < 0.70$, respectively (Sun 2013).

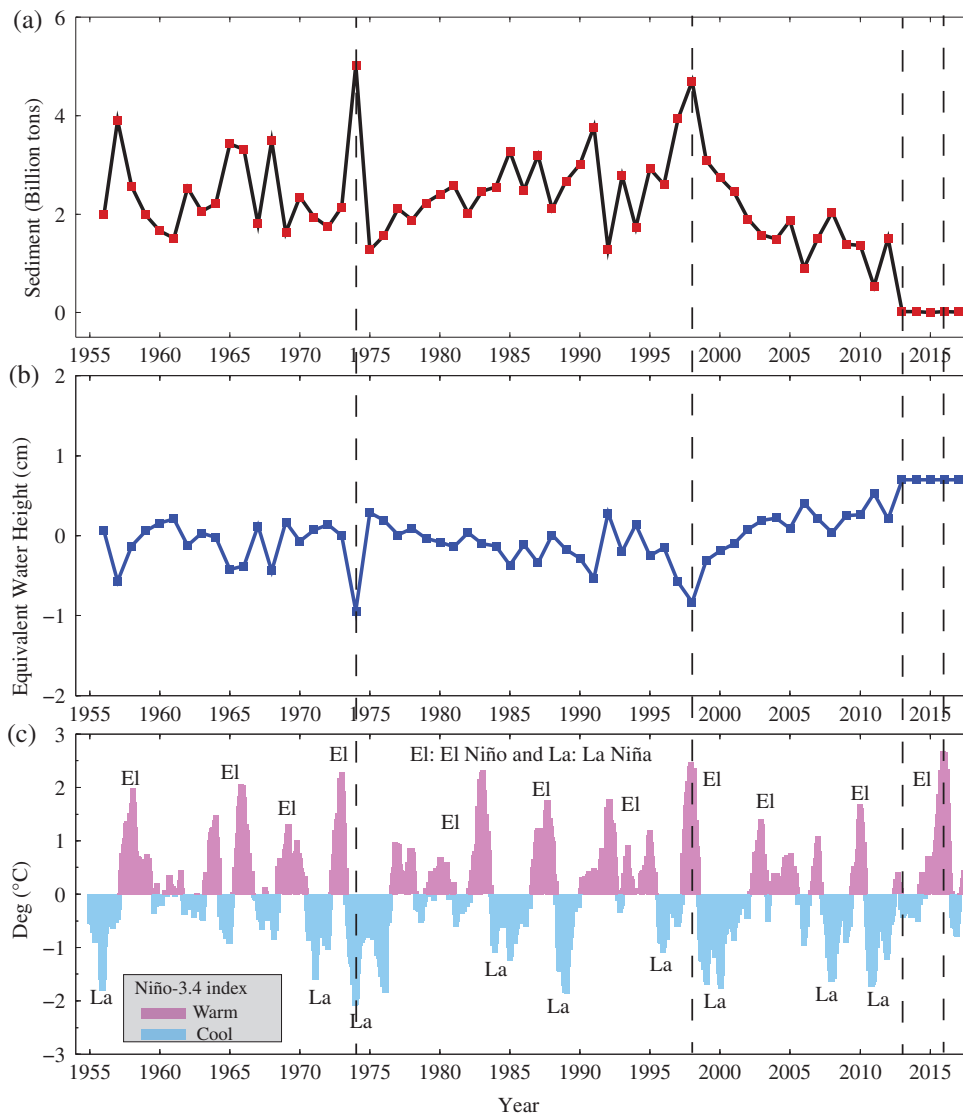


Figure 2. (a) Sediment transport from Pingshan and XJB stations; (b) sediment transport conversion to the equivalent water height; (c) the ENSO index (Niño-3.4) (Rayner et al. 2003).

Estimation of GWSC

Since the mass change caused by sediment transport can reach the level of billions of tons per year in JRB (Figure 2a), the estimation of LWSC from GRACE in our work includes not only the changes in groundwater storage and surface water but also sediment changes (SC). The GWSC from GRACE can be derived from the following formula:

$$\text{GWSC} = \text{LWSC} - (\text{SWSC} + \text{SMC} + \text{ICE} + \text{SC}) \quad (5)$$

where LWSC is from GRACE, SWSC is from in situ runoff data (Thomas and Famiglietti 2019); SMC is from GLDAS; ICE is the glacier mass change over JRB, and the value was -0.13 ± 0.07 cm/year during the period 2003 to 2015 from Xiang et al. (2016); SC is from in situ data (Figure 2b). Errors in the GWSC time series were estimated by propagating LWSC, SWSC, SMC, ICE, and SC errors. Moreover, HGWSC is from GRACE

subtracted SWSC, SMC, and climate-driven GWSC from CLM4.0 data.

Results

LWSC in JRB from GRACE Data

The accuracy of precipitation (P) and ET from different models data is assessed by comparing with in situ data. The precipitation from TRMM, GPCP, and four GLDAS models (NOAH, VIC, CLM, and MOS) are compared with in situ data. The precipitation information from in situ data uses the mean values of weather stations across JRB. The results (Figure 3b and Table S1) show that the precipitation data are consistent with data from weather stations across JRB, where the correlation coefficients are larger than 0.95, R^* is smaller than 0.5, NSE is larger than 0.8, and RMSE is approximately 2 cm. The highest accuracy of precipitation is TRMM,

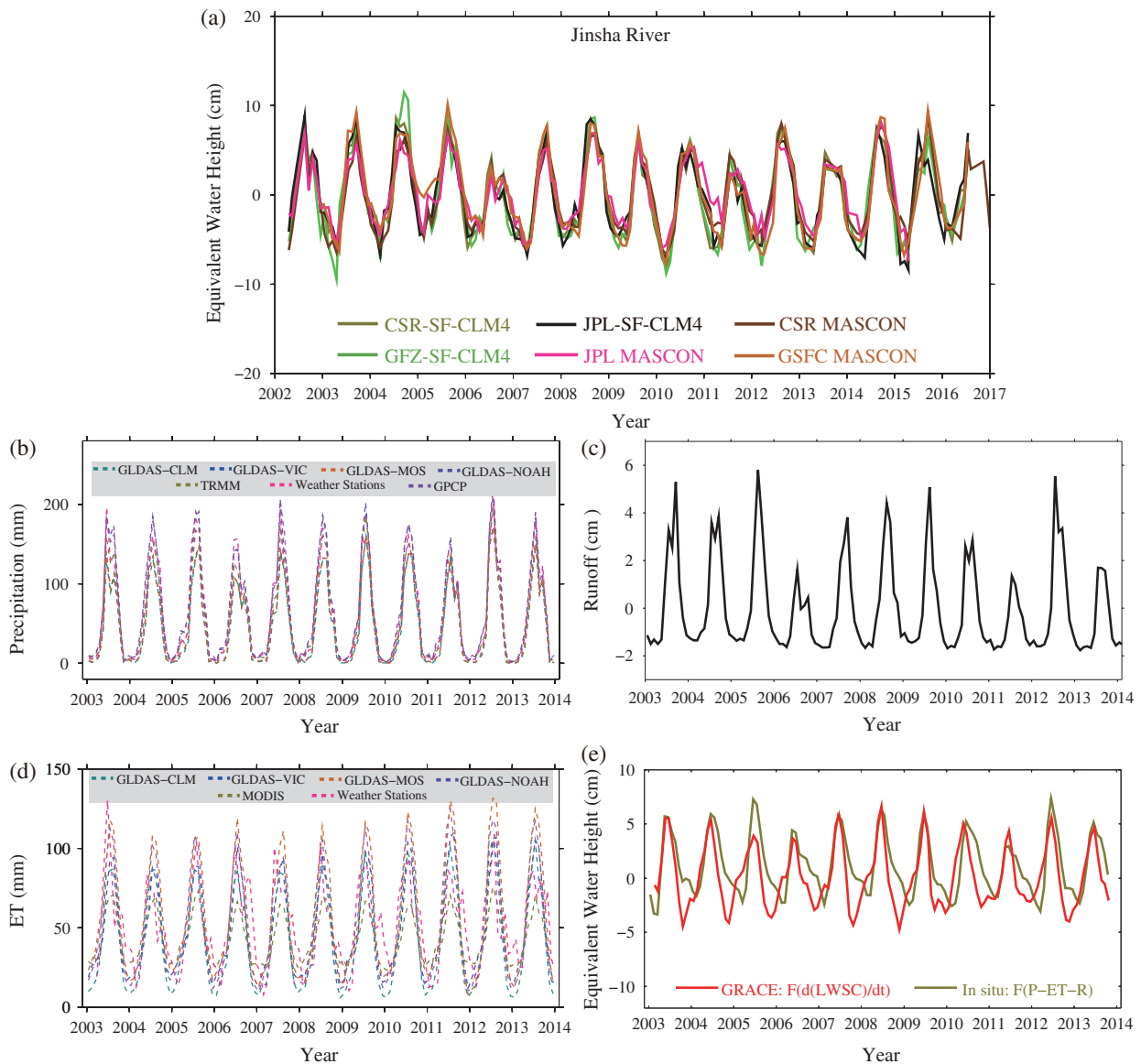


Figure 3. (a) LWSC from different GRACE products in JRB; (b) precipitation from weather stations, TRMM, GPCP, and four GLDAS models (NOAH, VIC, CLM, and MOS); (c) runoff data from Pingshan and XJB hydrological stations; (d) evapotranspiration (ET) from weather stations, MODIS, and four GLDAS models (NOAH, VIC, CLM, and MOS); (e) comparison between LWSC from GRACE data and in situ data based on (Equations 1, 2, and 3).

and the lowest is CLM. The ET from MODIS and the four GLDAS models are compared with in situ data. The results (Figure 3d and Table S2) show that the correlation between ET from in situ data and that of the models was poor, but the RMSE and NSE of the four GLDAS models are better than the MODIS results. To investigate the spatiotemporal variability of ET in JRB, here, the mean of the four GLDAS models' data is used.

LWSC are compared with GRACE from CSR, JPL, and GeoForschungsZentrum Postdam GFZ agencies using the SF and Mascons methods. From Figure 3a, the time series LWSC from different GRACE products compare favorably with each other regarding their temporal evolutions. The distinct seasonal variations were noted, with water storage maxima generally observed during the months of April and May and minima during

October and November. The trends of LWSC in JRB increased.

The results from water balance equations (Equations 1, 2, and 3) are shown in Figure 3e. Figure 3c shows the runoff data from Pingshan and XJB hydrological stations. From Figure 3e and Table 3, the correlation coefficients, RMSE, and NSE are nearly 0.8, 2 cm, and 0.8, respectively. LWSC from JPL Mascons RL06 performs well and shows the best accuracy in JRB.

Period, Trend, and Long-Term Change of Each LWSC Component in JRB

The original signal of LWSC can be represented as the sum of the long-term component, the period and the remaining residuals (Humphrey et al. 2016). The time series can be fitted by using the nonlinear least

Table 3**Statistical Results of LWSC Based on Equations 1, 2, and 3 during 2003 to 2013**

Method	Data	RMSE		Correlation	MAE	NSE
		(cm)	R^*	Coefficients	(cm)	
SF	CSR	2.04	1.18	0.81	1.53	0.79
	JPL	1.99	1.30	0.83	1.52	0.80
	GFZ	2.12	1.06	0.80	1.56	0.77
Mascon	CSR	1.80	1.44	0.84	1.51	0.83
	JPL	1.67	1.74	0.82	1.48	0.88
	GSFC	1.75	1.17	0.80	1.50	0.85

square method, including the linear trend, interannual, and semiannual cycles, and the remaining residuals. The time interval of LWSC is monthly, so a 13-month window moving average is a reasonable choice for estimating the long-term component (i.e., interannual and secular). From Figures 4 and 5, the results show that: (1) There are obvious seasonal changes, with maxima in the summer for P , R , SMC, SWSC, GWSC, and HGWSC, but in the spring for ET. The maximum of P is in July, while SMC and LWSC lagged by 2 months with their maxima in September. The maxima of SWSC, GWSC, and HGWSC are in July, and ET in May; (2) The interannual and trend of LWSC, GWSC, and HGWSC increase, but P , R , SWSC, and SMC decrease, and ET is basically unchanged.

From Figure 6, the spatial distributions with the trend of P during the period 2003 to 2015 almost all decreased. In the western JRB, the decrease in LWSC trend was due to the glaciers melting in the QTP due to global warming (Song et al. 2015). Comparing GWSC and HGWSC showed that the decreased groundwater in Yunnan province, China led to a continuous drought in recent years, which is caused by climate change with decreased P . From Table 4, the trend of GWSC under and without accounting for sediment transport was 0.89 ± 0.11 and 0.76 ± 0.10 cm/year, respectively, during the period of 2003 to 2015. The contribution of SC to groundwater change is 15% [$=(0.89-0.76)/0.89*100$], showing that sediment transport should be accounted for in GWSC across JRB. In addition, the climate-driven groundwater change was about -0.09 ± 0.14 cm/year (the difference between the results of GWSC and HGWSC trends), which was in agreement with the negative precipitation, runoff, and soil moisture trends.

There is a high degree of correlation between P , R , and SC, and a certain correlation between LWSC and GWSC, ET and SMC, GWSC and HGWSC, and GWSC and SC (Table S3). Moreover, there is no correlation between each component and Niño-3.4, MOI, or NAO during the period 2003 to 2013 (Table S4). Based on the above results, (1) there is a high correlation between SC, P , and R , and there is a certain correlation between sediment and LWSC, GWSC, and HGWSC, showing that sediment transport can influence GWSC; (2) SMC

is mainly affected by runoff and ET, which means that the larger R follows the larger SMC, and the larger ET with the smaller runoff, and vice versa; and (3) there are high correlations among LWSC, GWSC, and HGWSC, showing that LWSC in JRB mainly comes from GWSC, and GWSC may be mainly affected by human activities.

Discussion

The Effect of Dams and Climate Changes on the GWSC in JRB

Zhang et al. (2012) concluded that the construction of large-scale reservoirs in JRB was an important factor in declining sediment yields since the 1990s. Li et al. (2018) found that the average annual sediment transport in JRB decreased 75.9% from 2011 to 2015 because of the operation of the cascade reservoirs in the middle JRB since 2010. The construction of new dams, such as the XJB Reservoir (2012) and the XLD Reservoir (2013) in the lower JRB and many other cascade reservoirs since 2010 in the middle JRB, further decreased the sediment transport by 58.5% (BHT) and 83.8% (XJB) recently, in the 5 years from 2011 to 2015, and sediment transport will continue to reduce due to the construction of more dams in the future. From Figure 2a-c, due to the ENSO events, the sediment transport abruptly increased during 1973 to 1974 and 1997 to 1998. However, the sediment transport remarkably reduced after 2000, and has reached almost zero since 2013, although there was an ENSO event during 2015 to 2016. This was mainly due to the beginning of water impoundment in the XJB reservoir since 2012, which led to nearly zero sediment transport after 2012. The sediment transport was mainly affected by human activities (damming) after 2000 although it was also affected by the river's water cycles. With the increased number of reservoirs, this will have profound impact on the river's water cycles. Artificial cascade reservoirs can trap sediment in the reservoirs, leading to sediment transport decrease. The sediment mass is stored in the artificial reservoirs. The increased sediment mass is also included in LWSC from GRACE. Therefore, the assessment of GWSC by using GRACE data should account for the sediment transport in the river basin with plenty of reservoirs.

Xiang et al. (2016) showed the GWSC without accounting for SC in JRB also increased and pointed to the melted water from the glaciers/snow caps and permafrost in the Heng-duan Mountains, with increased air temperature conditions during the period 2003 to 2009 as the reason for the increasing trend. Here, it was found that the increasing trend of GWSC during the period of 2003 to 2015 may be due to increased artificial cascade reservoirs. The purpose of the construction of artificial cascade reservoirs is to generate hydropower or to store water for agriculture and industry. Due to the sparse population and almost no irrigation in JRB, the main purpose of artificial cascade reservoirs

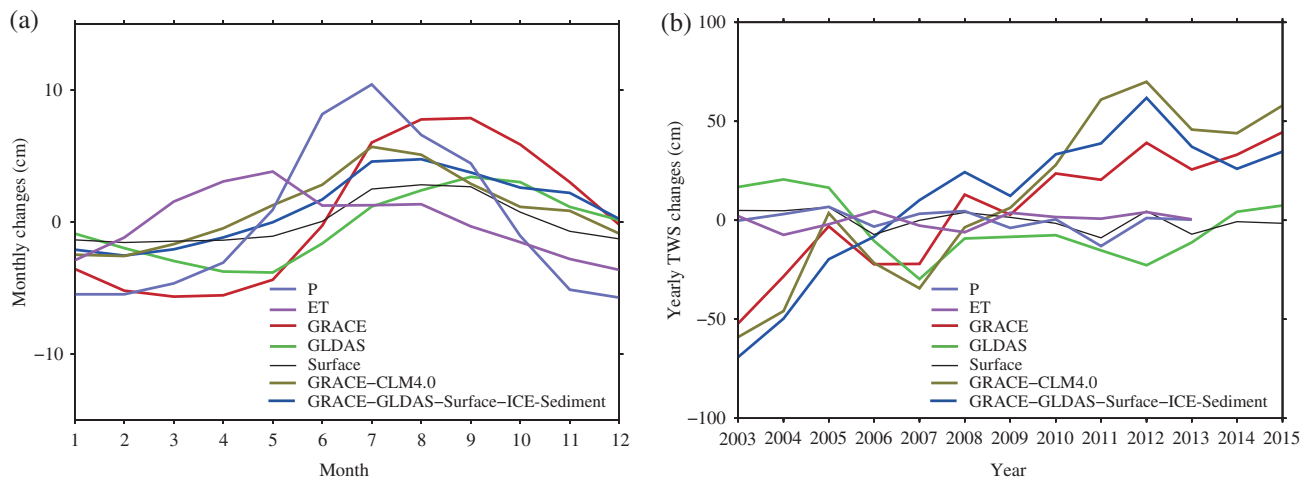


Figure 4. (a) Monthly and (b) total annual changes in different hydrological variables.

in JRB is to generate hydropower, and transmit to the eastern China through the West Power to East project for supporting social and economic development. Over the Jinsha River hydropower bases, XJB is the only dam with considering irrigation in the 25 hydropower stations of Jinsha River hydropower bases, and the remaining 24 dams have no irrigation and water conservancy facilities, and only for generating electricity. In addition, the increasing of groundwater storage mainly occurs in the reservoir area, and the area occupied by the dam itself can be neglected comparing with the inundation area in the reservoir. The local groundwater reduction caused by concrete dam impervious area can also be neglected. Although the reservoir sluicing during the flood is relatively concentrated (large releasing flow), it is much lower than the flood through the nature river. Overall, the time of the water retention in the reservoir is much longer than that in the natural river. The retention time can be calculated as the water storage capacity divided by the averaged river cross-section area and the averaged flow velocity. It can be seen that the larger the water storage capacity, the smaller the flow rate after impoundment, and the longer water retention in the reservoir, which increases the infiltration time and the groundwater. Therefore, the stored water in artificial cascade reservoirs will percolate downward, which may have caused the GWSC increase. However, more in situ data should be used to investigate in the future, such as those from wells.

Uncertainty of GWSC Assessment in JRB

In this study, the spatiotemporal variability of groundwater storage in JRB is derived, showing that the line trend of LWSC was 0.76 ± 0.10 cm/year during the period of 2003 to 2015 from GRACE and other data. The sum of ICE, SWSC, SMC, and GWSC should equal to LWSC (Table 4) based on the water balance theory, but they were also different. The results were obtained from different data sources, which all had errors and uncertainties.

Although there is uncertainty in the results and no wells data to verify, this study considers all uncertainties and quantifies them. Moreover, LWSC and GWSC are compared with the results from Changjiang Rivers Water Resources Bulletin (CWRB) (<http://www.cjw.gov.cn/zwzc/bmgb/>). From Figure 7, LWSC and GWSC from GRACE agree well with the results from CWRB with the correlation coefficient over 0.9. In addition, Joodaki et al. (2014) assessed groundwater changes in the Middle East using the same processing strategy as that used in this paper and verified the results with data observed from wells in Iran. This work also suggests that remote sensing GRACE and model data jointly provide another effective method for understanding hydrological processes in sparsely populated areas.

GRACE and other remote sensing tasks cannot replace ground-based hydrological observations now, but they provide a unique approach to global water resource management. With the development of satellite technology, regional and global hydrological models obtained by means of satellite observation will better serve the management of water resources (Famiglietti et al. 2011). Combined hydrological remote sensing observations, hydrological models, and existing high-precision hydrological station observations can provide a wide range of high-precision available freshwater maps for a particular region or the entire world. This kind of scientific research is essential for more efficient, sustainable, and cross-boundary water resources cooperation management.

Limitations of GWSC from GRACE Data

The successful launch of the GRACE satellites has provided considerable support for monitoring GWSC, but many limitations still need to be overcome. The most serious shortage is the low temporalspatial resolution of the GRACE mission (Rodell et al. 2018), revealing that (1) the GRACE data have north-south stripe noise (Wahr et al. 1998), which requires filter and signal attenuation (Landerer and Swenson 2012); (2) LWSC from GRACE

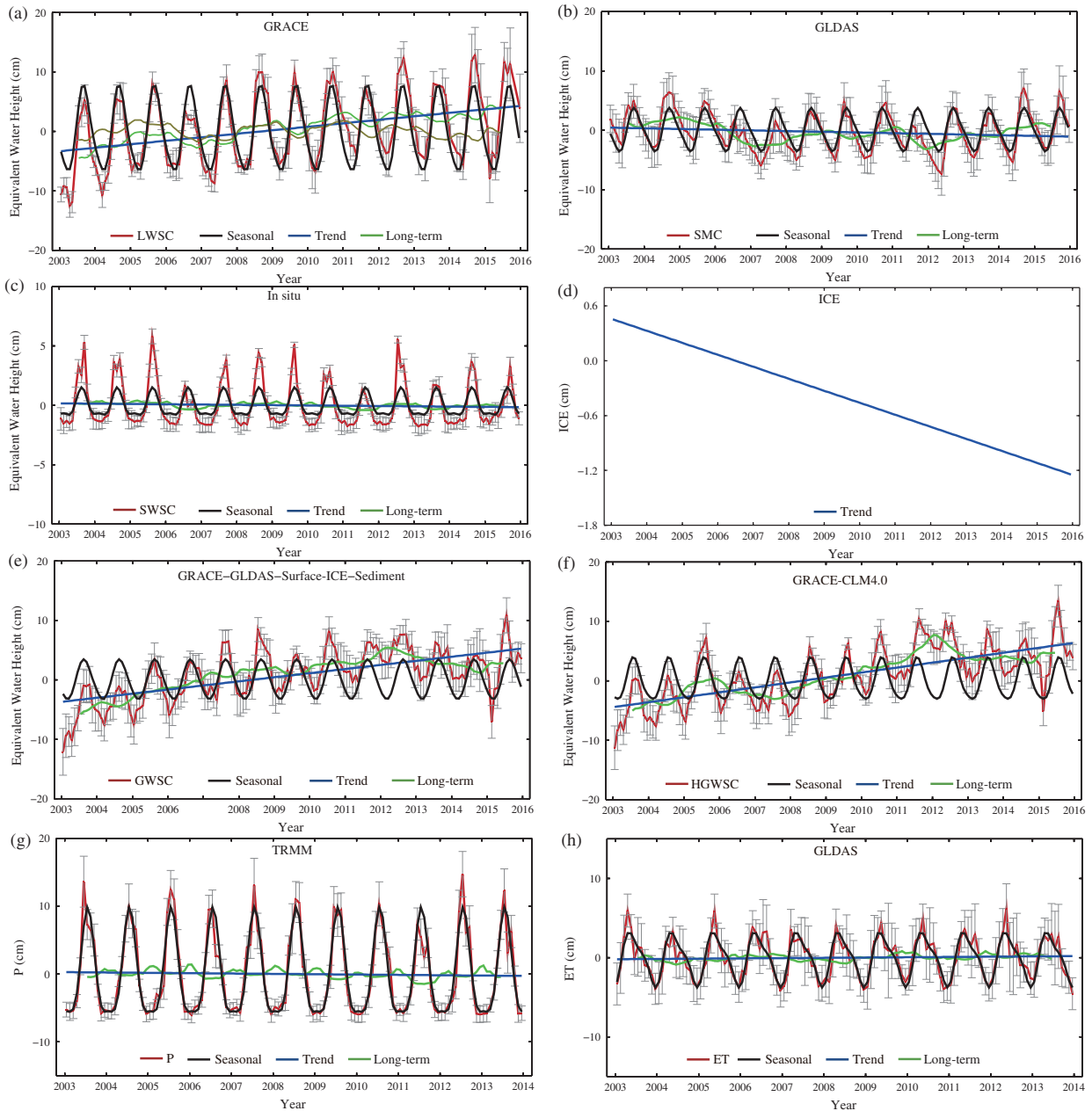


Figure 5. Different hydrological variables with uncertainties, and their seasonal, trend, and long-term changes. (a) LWSC, (b) SMC, (c) SWSC, (d) ICE, (e) GWSC, (f) HGWSC, (g) P, (h) ET. Note ICE is only the result of trend.

data are the total water storage change, including snow, surface water, soil moisture, and groundwater storage, which cannot be isolated using GRACE data alone (Sun et al., 2019). There are errors in the background model and hydrological data, which can also affect the results of GWSC.

Additionally, it is clear that most basins in the world are small for GRACE resolution ($\approx 160,000 \text{ km}^2$). However, the results from Lorenz et al. (2014) supported the fact that the spatial resolution of the GRACE mission was not the only critical factor for studying water resources. They cited the signal strength as another determinant and termed it the “gravimetric resolution.” The latest results from Yi et al. (2017) showed that the

signal of a small ($\sim 0.2^\circ \times 0.2^\circ$) reservoir can potentially be detected by GRACE data if the mass change is larger than 6 Gt. Therefore, it is necessary to further study an effective method to improve the temporal-spatial resolution of GWSC detected from GRACE data, especially in the small basins. On the other hand, due to lack in situ data (such as wells), it is very hard to verify the GWSC from GRACE data.

Conclusions

GWSC are investigated, accounting for sediment transport by decomposing LWSC from GRACE data, hydrologic models, and in situ data. The periods, trends, and interannual changes of each LWSC component, such

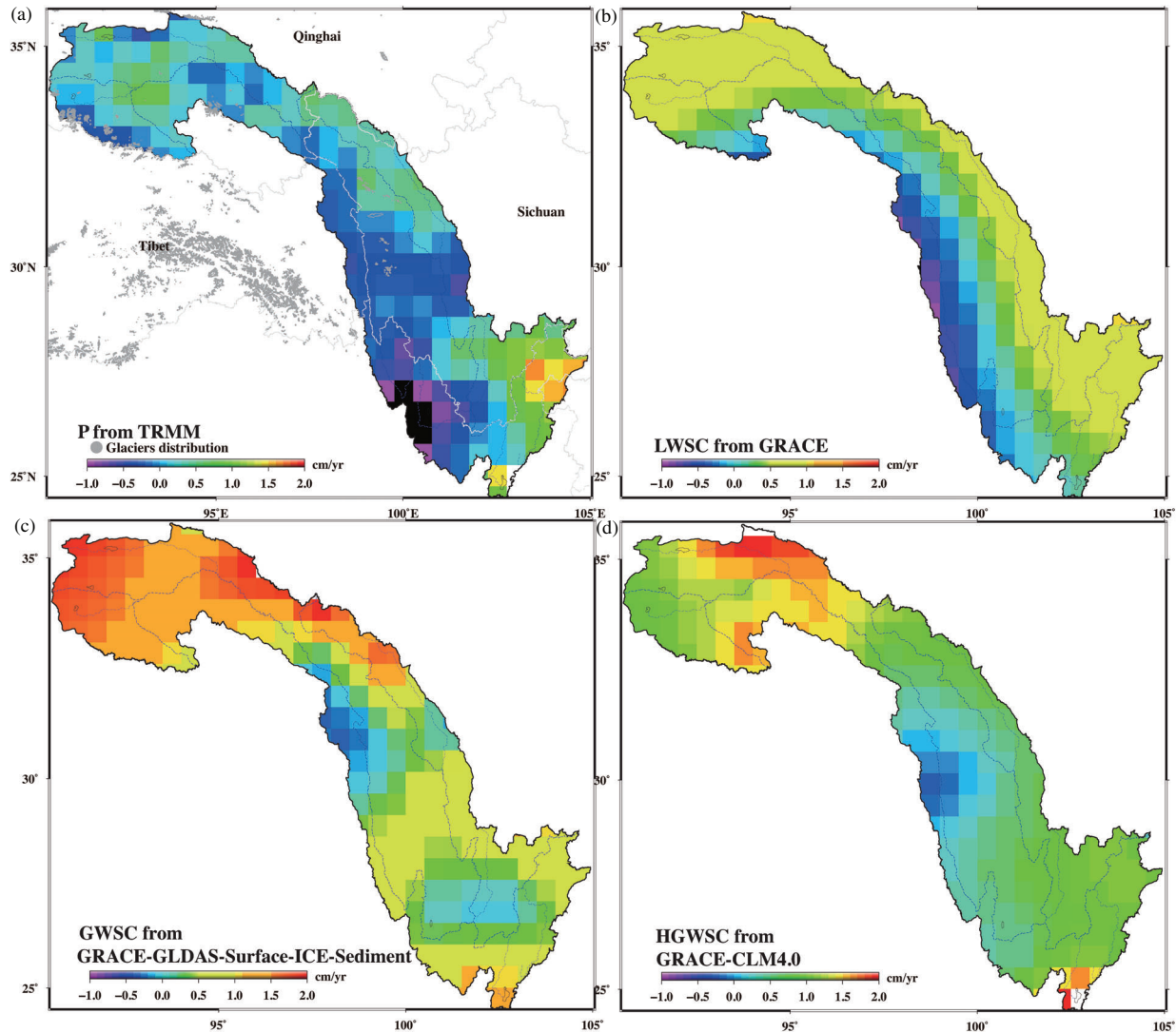


Figure 6. Spatial distributions with trends of (a) P , (b) LWSC, (c) GWSC, and (d) HGWSC in JRB during the period 2003 to 2015.

Table 4
Trends of Each Hydrological Variable during the Period 2003 to 2015

Hydrological Variables	Time	Trend (cm/year)
P	2003 to 2013	-0.02 ± 0.17
ET	2003 to 2013	0.00 ± 0.08
R	2003 to 2013	-0.02 ± 0.04
LWSC	2003 to 2015	0.52 ± 0.12
SMC	2003 to 2015	-0.19 ± 0.06
ICE	2003 to 2015	-0.13 ± 0.07
GRACE-GLDAS-Surface-ICE	2003 to 2015	0.89 ± 0.11
GRACE-GLDAS-Surface-ICE- Sediment	2003 to 2015	0.76 ± 0.10
GRACE-CLM4.0	2003 to 2015	0.85 ± 0.08
SC	2003 to 2015	0.03 ± 0.01

as SMC, SWSC, and GWSC, are analyzed. The key findings are listed as follows:

- 1 There are different accuracies in different precipitation data, but the six precipitation data of MODIS and the four GLDAS models (NOAH, VIC, CLM, and MOS) show good correlation in JRB. The best precipitation data are TRMM, and there are few differences among the four GLDAS models in the precipitation data across JRB. There is a large difference with different ET data, and these data have large uncertainties in JRB. LWSC from different GRACE products agreed well with each other and have correlation coefficients larger than 0.8, RMSE of nearly 2 cm, and NSE of nearly 0.8, but LWSC from JPL Mascons 06 shows the best agreement, with the lowest RMSE and the largest NSE.
- 2 The trend of GWSC when accounting for sediment transport in JRB was 0.76 ± 0.10 cm/year, and without accounting for sediment transport was 0.89 ± 0.11 cm/year, during the period 2003 to 2015. The trend of GWSC when accounting for sediment transport in JRB compared to without accounting for sediment transport is decreased by approximately

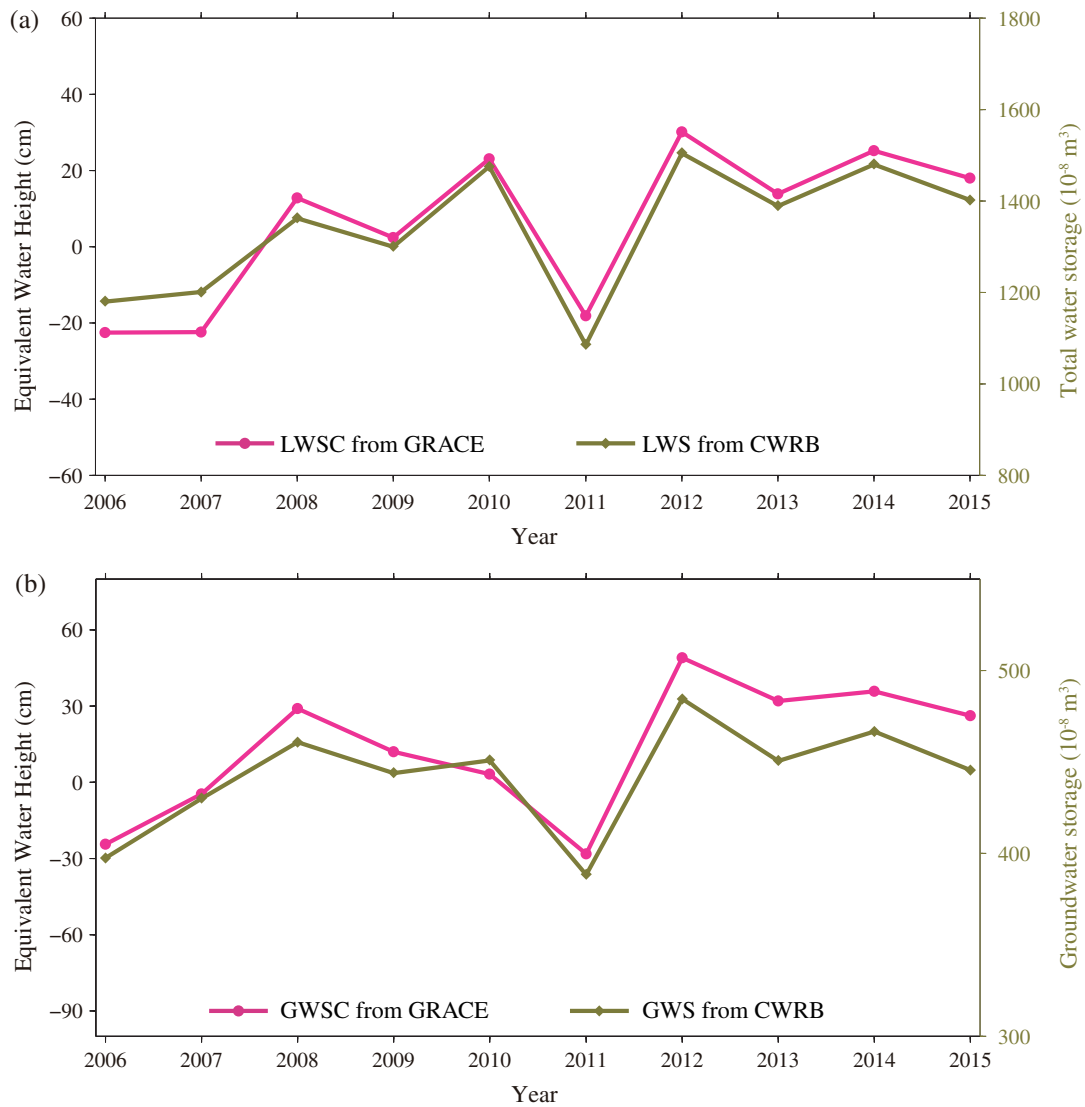


Figure 7. Comparing the LWSC (a) and GWSC (b) from GRACE, and CWRB data.

- 0.13 cm/year, and the contribution of sediment transport accounts for 15%.
- 3 LWSC, SMC, and GWSC show a clear seasonal cycle with maxima in summer and minima in winter. The interannual variability of GWSC increased during the period 2003 to 2015.
 - 4 Changes in groundwater contribute most to LWSC and are controlled by human activities, such as future dam constructions across JRB, and climate variations (such as snow and glacier melt due to increased temperatures).

In this study, we investigate the GWSC accounting for sediment mass change, LWSC, SMC, SWSC, P , and ET in the upper mountainous basin of JRB. The results are useful for improving the estimation of hydrologic variables. The method in this study can be reproduced in other parts of the world in order to acquire similar conclusions and to improve the understanding of hydrological processes.

With the development of satellite technology, such as the ICESat-2 (Abdalati et al. 2010; it was launched on September 15, 2018), and the GRACE Follow-On mission (Flechtner et al. 2014; it was launched on May 22, 2018), satellite observations will be better utilized to investigate water storage. Moreover, the quantitative estimation of the hydrological variables for each river basin using multisource satellite observations is crucial to understand land water cycles and benefit global and regional water resource management.

Acknowledgment

The authors thank the following data providers for making the data available: GRACE, GLDAS, runoff, in situ water level, TRMM, GPCP, Climate indices, and National Meteorological Information Center and CLM4.0 from Prof. Lo Minhui. This study is supported by the NSFC (China) under Grants 41974019, 41704011, 41674015, 41974007, 41774019, 41771449,

41874093, and 41474018; supported by the CRSRI Open Research Program (Program SN:CKWV2019728/KY); The National key research and development program of China under Grant 2016YFB0501702. We also sincerely thank Editor-in-Chief, Executive Editor, Associated Editor, and two anonymous reviewers for their insightful and constructive comments on this article, which have greatly helped improving previous versions of this manuscript.

Authors' Note: The author(s) does not have any conflicts of interest.

Supporting Information

Additional supporting information may be found online in the Supporting Information section at the end of the article. Supporting Information is generally *not* peer reviewed.

Table S1 Statistical results of precipitation from different data.

Table S2. Statistical results of evapotranspiration (ET) from different data.

Table S3. The correlation among the P , ET , R (Surface water), $LWSC$, SMC , $GWSC$, $HGWSC$ and $Sediment$ change (SC).

Table S4. The correlation among each hydrological variables and Niño-3.4, MOI , and NAO .

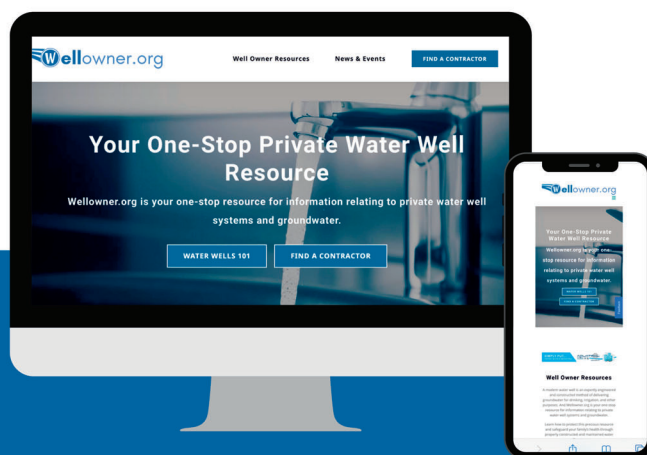
References

- Abdalati, W., H.J. Zwally, R. Bindenschadler, B. Csatho, S.L. Farrell, H.A. Fricker, D. Harding, R. Kwok, M. Lefsky, and T. Markus. 2003. The version-2 global precipitation climatology project (GPCP) monthly precipitation analysis (1979–present). *Journal of Hydrometeorology* 4, no. 6: 1147–1167.
- Abdalati, W., H.J. Zwally, R. Bindenschadler, B. Csatho, S.L. Farrell, H.A. Fricker, D. Harding, R. Kwok, M. Lefsky, T. Markus, A. Marshak, T. Neumann, S. Palm, B. Schutz, B. Smith, J. Spinhirne, and C. Webb. 2010. The ICES at-2 laser altimetry mission. *Proceedings of the IEEE* 98, no. 5: 735–751. <https://doi.org/10.1109/JPROC.2009.2034765>
- Adler, R.F., G.J. Huffman, A. Chang, R. Ferraro, P. Xie, J. Janowiak, B. Rudolf, U. Schneider, S., Curtis, D. David, A. Gruber, J. Susskind, P. Arkin, E. Nelkin. 2003. The version-2 global precipitation climatology project (GPCP) monthly precipitation analysis (1979–present). *Journal of Hydrometeorology* 4, no. 6: 1147–1167. [https://doi.org/10.1175/1525-7541\(2003\)004<1147:TVGP-CP>2.0.CO;2](https://doi.org/10.1175/1525-7541(2003)004<1147:TVGP-CP>2.0.CO;2)
- Alley, W.M., B.R. Clark, D.M. Ely, and C.C. Faunt. 2018. Groundwater development stress: Global-scale indices compared to regional modeling. *Ground Water* 56, no. 2: 266–275.
- Alley, W.M., R.W. Healy, J.W. LaBaugh, and T.E. Reilly. 2002. Flow and storage in groundwater systems. *Science* 296, no. 5575: 1985–1990.
- Als Dorf, D.E., E. Rodríguez, and D.P. Lettenmaier. 2007. Measuring surface water from space. *Reviews of Geophysics* 45, no. 2: RG2002.
- Bonan, G.B., P.J. Lawrence, K.W. Oleson, S. Levis, M. Jung, M. Reichstein, D.M. Lawrence, and S.C. Swenson. 2011. Improving canopy processes in the community land model version 4 (CLM4) using global flux fields empirically inferred from FLUXNET data. *Journal of Geophysical Research* 116, no. G2.
- Castle, S.L., B.F. Thomas, J.T. Reager, M. Rodell, S.C. Swenson, and J.S. Famiglietti. 2014. Groundwater depletion during drought threatens future water security of the Colorado River basin. *Geophysical Research Letters* 41, no. 16: 5904–5911.
- Chang, J., J. Wei, Y. Wang, M. Yuan, and J. Guo. 2017. Precipitation and runoff variations in the Yellow River Basin of China. *Journal of Hydroinformatics* 19, no. 1: 138–155.
- Chao, N., Z. Luo, Z. Wang, and T. Jin. 2018. Retrieving groundwater depletion and drought in the Tigris-Euphrates Basin between 2003 and 2015. *Groundwater* 56, no. 5: 770–782.
- Cheng, M., J. Ries, and B. Tapley. 2011. Variations of the Earth's Fig. Axis from satellite laser ranging and GRACE. *Journal of Geophysical Research* 116, no. B1. <https://doi.org/10.1029/2010JB000850>
- Famiglietti, J.S., Murdoch, L., Lakshmi, V., and Arrigo J. 2011. Establishing a framework for community modeling in hydrologic science. Report from the 3rd Workshop on a Community Hydrologic Modeling Platform (CHyMP): A Strategic and Implementation Plan, Technical Report 10, March 15–17, Irvine, CA. <https://doi.org/10.4211/techrpts.20110317.tr10>.
- Feng, W., C.K. Shum, M. Zhong, and Y. Pan. 2018. Groundwater storage changes in China from satellite gravity: An overview. *Remote Sens* 10(5), 674. <https://doi.org/10.3390/rs10050674>
- Flechtner, F., P. Morton, M. Watkins, and F. Webb. 2014. Status of the GRACE follow-on mission. *IAG Symposium Gravity, Geoid, and Height Systems* 141, no. 1: 117–121.
- Forootan, E., R. Rietbroek, J. Kusche, M.A. Sharifi, J.L. Awange, M. Schmidt, P. Omondi, and J.S. Famiglietti. 2014. Separation of large scale water storage patterns over Iran using GRACE, altimetry and hydrological data. *Remote Sensing of Environment* 140, no. 2014: 580–595.
- Forootan, E., A. Safari, A. Mostafaie, M. Schumacher, M. Delavar, and J.L. Awange. 2016. Large-scale total water storage and water flux changes over the arid and semiarid parts of the Middle East from GRACE and reanalysis products. *Surveys in Geophysics* 38, no. 3: 591–615. <https://doi.org/10.1007/s10712-016-9403-1>
- Frappart, F., F. Papa, A. Güntner, J. Tomasella, J. Pfeffer, G. Ramillien, T. Emilio, J. Schietti, L. Seoane, J. da Silva Carvalho, D. Medeiros Moreira, M.P. Bonnet, and F. Seyler. 2019. The spatio-temporal variability of groundwater storage in the Amazon River Basin. *Advances in Water Resources* 124, no. 1: 41–52. <https://doi.org/10.1016/j.advwatres.2018.12.005>
- Frappart, F., and G. Ramillien. 2018. Monitoring groundwater storage changes using the gravity recovery and climate experiment (GRACE) satellite mission: A review. *Remote Sensing* 10, no. 6: 829.
- Gleeson, T., K.M. Befus, S. Jasechko, E. Luijendijk, and M.B. Cardenas. 2016. The global volume and distribution of modern groundwater. *Nature Geoscience* 9, no. 2: 161.
- Hanjra, M.A., and M.E. Qureshi. 2010. Global water crisis and future food security in an era of climate change. *Food Policy* 35, no. 5: 365–377. <https://doi.org/10.1016/j.foodpol.2010.05.006>
- Hasanean, H.M. 2004. *Middle East Meteorology*. Paris, France: UNESCO-EOLSS Joint Committee Secretariat.
- Huffman, G.J., R.F. Adler, D.T. Bolvin, G. Gu, E.J. Nelkin, and K.P. Bowman. 2007. The TRMM multi-satellite precipitation analysis: Quasi-global, multi-year, combined-sensor precipitation estimates at fine scale. *Journal of Hydrometeorology* 8, no. 1: 38–55. <https://doi.org/10.1175/JHM560.1>

- Humphrey, V., L. Gudmundsson, and S.I. Seneviratne. 2016. Assessing global water storage variability from GRACE: Trends, seasonal cycle, subseasonal anomalies and extremes. *Surveys in Geophysics* 37, no. 2: 357–395. <https://doi.org/10.1007/s10712-016-9367-1>
- Ireson, A., C. Makropoulos, and C. Maksimovic. 2006. Water resources modelling under data scarcity: Coupling MIKE BASIN and ASM groundwater model. *Water Resources Management* 20, no. 4: 567–590.
- Joodaki, G., J. Wahr, and S. Swenson. 2014. Estimating the human contribution to groundwater depletion in the Middle East, from GRACE data, land surface models, and well observations. *Water Resources Research* 50, no. 3: 2679–2692.
- Landerer, F.W., and S.C. Swenson. 2012. Accuracy of scaled GRACE terrestrial water storage estimates. *Water Resources Research* 48, no. 4: W0453111. <https://doi.org/10.1029/2011WR011453>
- Li, D., X. Lua, X. Yang, L. Chen, and L. Lin. 2018. Sediment load responses to climate variation and cascade reservoirs in the Yangtze River: A case study of the Jinsha River. *Geomorphology* 322, no. 1: 41–52.
- Lin, M., A. Biswas, and E.M. Bennett. 2019. Spatio-temporal dynamics of groundwater storage changes in the Yellow River Basin. *Journal of Environmental Management* 235: 84–95. <https://doi.org/10.1016/j.jenvman.2019.01.016>
- Long, D., Y.J. Shen, A. Sun, Y. Hong, L. Longueuevigne, Y.T. Yang, B. Li, and L. Chen. 2014. Drought and flood monitoring for a large karst plateau in Southwest China using extended GRACE data. *Remote Sensing of Environment* 155, no. 2014: 145–160.
- Lorenz, C., B. Devaraju, M.J. Tourian, J. Riegger, H. Kunstmann, and N. Sneeuw. 2014. Large-scale runoff from landmasses: A global assessment of the closure of the hydrological and atmospheric water balances. *Journal of Hydrometeorology* 15, no. 6: 2111–2139.
- Luthcke, S.B., T.J., Sabaka, B.D., Loomis, A.A., Arendt, J.J., McCarthy, J., Camp. 2013. Antarctica, Greenland and Gulf of Alaska land ice evolution from an iterated GRACE global mascon solution. *J. Glaciol.*, 59, 613–631.
- Margat, J., and J. van de Gun. 2013. *Groundwater Around the World: A Geographic Synopsis*. Taylor & Francis, UK.
- Martin-Vide, J., and J.-A. Lopez-Bustins. 2006. The Western Mediterranean scillation and rainfall in the Iberian Peninsula. *International Journal of Climatology* 26, no. 11: 1455–1475. <https://doi.org/10.1002/joc.1388>
- Mu, Q., F.A. Heinsch, M. Zhao, and S.W. Running. 2007. Development of a global evapotranspiration algorithm based on MODIS and global meteorology data. *Remote Sensing of Environment* 111, no. 4: 519–536.
- Ndehedehe, C.E., J.L. Awange, N.O. Agutu, and O. Okwuashi. 2018. Changes in hydrometeorological conditions over tropical West Africa (1980–2015) and links to global climate. *Global and Planetary Change* 162, no. 2018: 321–341.
- Munier, S., M., Becker, P., Maisongrande, A., Cazenave. 2012. Using GRACE to detect groundwater storage variations: the cases of Canning basin and Guarani aquifer system. *International Water Technology Journal*, 2, 2–13.
- Oki, T., and S. Kanae. 2006. Global hydrological cycles and world water resources. *Science* 313, no. 5790: 1068–1072.
- Peltier, W.R., D.F. Argus, and R. Drummond. 2015. Space geodesy constrains ice age terminal deglaciation: The global ICE-6G_C (VM5a) model. *Journal of Geophysical Research - Solid Earth* 120, no. 1: 450–487.
- Peltier, W.R., D.F. Argus, and R. Drummond. 2017. Comment on “An Assessment of the ICE-6G_C B1(VM5a) glacial isostatic adjustment model by Purcell et al. 2017”. *Journal of Geophysical Research - Solid Earth* 122: 2019–2028.
- Rast, M., J. Johannessen, and W. Mauser, 2014. Review of understanding of Earth’s hydrological cycle: observations, theory and modelling. *Surv. Geophys.* 35 (3), 491–513.
- Rayner, N.A., D.E. Parker, E.B. Horton, C.K. Folland, L.V. Alexander, D.P. Rowell, E.C. Kent, and A. Kaplan. 2003. Global analyses of sea surface temperature, sea ice, and night marine air temperature since the late nineteenth century. *Journal of Geophysical Research* 108, no. D14: 4407. <https://doi.org/10.1029/2002JD002670>
- Richey, A.S., B.F. Thomas, M.-H. Lo, J.S. Famiglietti, J.T. Reager, K. Voss, S. Swenson, and M. Rodell. 2015. Quantifying renewable groundwater stress with GRACE. *Water Resources Research* 51, no. 7: 5217–5238. <https://doi.org/10.1002/2015WR017349>
- Rodell, M., J. Chen, H. Kato, J.S. Famiglietti, J. Nigro, and C.R. Wilson. 2007. Estimating groundwater storage changes in the Mississippi River basin (USA) using GRACE. *Hydrogeology Journal* 15, no. 1: 159–166.
- Rodell, M., J.S. Famiglietti, J. Chen, S.I. Seneviratne, P. Viterbo, S. Holl, C.R. Wilson. 2004. Basin scale estimates of evapotranspiration using GRACE and other observations. *Geophysical Research Letters* 31, no. 20: L20504. <https://doi.org/10.1029/2004GL020873>
- Rodell, M., J.S. Famiglietti, D.N. Wiese, J.T. Reager, H.K. Beaudoin, F.W. Landerer, and M.H. Lo. 2018. Emerging trends in global freshwater availability. *Nature* 557, no. 7707: 651–659. <https://doi.org/10.1038/s4158601801231>
- Rodell, M., I. Velicogna, and J.S. Famiglietti. 2009a. Satellite-based estimates of groundwater depletion in India. *Nature* 460, no. 7258: 999–1002.
- Rodell, M., I. Velicogna, and J.S. Famiglietti. 2009b. Satellite-based estimates of groundwater depletion in India. *Nature* 460, no. 7258: 999–1002.
- Rogers, J.C. 1984. The association between the North Atlantic Oscillation and the Southern Oscillation in the northern hemisphere. *Monthly Weather Review* 112: 1999–2015.
- Save, H., S.Bettadpur, and B.D.Tapley. 2016. High resolution CSR GRACE RL05 mascons, *J. Geophys. Res. Solid Earth*, 121 (10), 7547–7569, doi:10.1002/2016JB013007.
- Schlosser, C.A., K. Strzepek, X. Gao, C. Fant, E. Blanc, S. Paltsev, H. Jacoby, J. Reilly, and A. Gueneau. 2014. The future of global water stress: An integrated assessment. *Earths Future* 2, no. 8: 341–361.
- Seiler, K.P., and J.R. Gat. 2007. *Groundwater Recharge from Run-off, Infiltration and Percolation*, 248. Springer: Berlin, Germany. <https://doi.org/10.1007/978-1-4020-5306-1>
- Song, C.Q., L.H. Ke, B. BoHuang, and K.S. Richards. 2015. Can mountain glacier melting explain the GRACE-observed mass loss in the southeast Tibetan Plateau: From a climate perspective? *Global and Planetary Change* 124: 1–9.
- Sun, A.Y. 2013. Predicting groundwater level changes using GRACE data. *Water Resources Research* 49, no. 9: 5900–5912.
- Sun, A.Y., B. R., Scanlon, Z., Zhang, D., Walling, S.N., Bhanja, A., Mukherjee, Z., Zhong. 2019. Combining physically based modeling and deep learning for fusing GRACE satellite data: Can we learn from mismatch? *Water Resour. Res.*, 55 (9), 1179–1195.
- Swenson, S., and J. Wahr. 2006. Estimating large-scale precipitation minus evapotranspiration from GRACE satellite gravity measurements. *Journal of Hydrometeorology* 7, no. 2: 252–269. <https://doi.org/10.1175/JHM478.1>
- Swenson, S.C., D.P. Chambers, and J. Wahr. 2008. Estimating geocenter variations from a combination of GRACE and ocean model output. *Journal of Geophysical Research* 113, no. B8. <https://doi.org/10.1029/2007JB005338>
- Tapley, B.D., S. Bettadpur, J. Ries, P.F. Thompson, and M. Watkins. 2004. GRACE measurements of mass variability in the Earth system. *Science* 305, no. 5683: 503–505.

- Thomas, B.F., and J.S. Famiglietti. 2019. Identifying climate-induced groundwater depletion in GRACE observations. *Scientific Reports* 9, no. 1: 4124.
- Voss, K.A., J.S. Famiglietti, M. Lo, C. Linage, M. Rodell, and S.C. Swenson. 2013. Groundwater depletion in the Middle East from GRACE with implications for transboundary water management in the Tigris-Euphrates-Western Iran region. *Water Resources Research* 49, no. 2: 904–914. <https://doi.org/10.1002/wrcr.20078>
- Wahr, J., M. Molenaar, and F. Bryan. 1998. Time variability of the Earth's gravity field: Hydrological and oceanic effects and their possible detection using GRACE. *Journal of Geophysical Research* 103, no. B12: 30205–30229.
- Wiese, D.N., F.W., Landerer, M.M., Watkins. 2016. Quantifying and reducing leakage errors in the JPL RL05M GRACE mascon solution. *Water Resour. Res.*, 52, 7490–7502.
- Xiang, L., H. Wang, H. Steffen, P. Wu, L. Jia, L. Jiang, Q. Shen. 2016. Groundwater storage changes in the Tibetan lateau and adjacent areas revealed from GRACE satellite gravity data. *Earth and Planetary Science Letters* 449, no. 1: 228–239.
- Yi, S., C. Song, Q. Wang, L. Wang, K. Heki, and W. Sun. 2017. The potential of GRACE gravimetry to detect the heavy rainfall-induced impoundment of a small reservoir in the upper Yellow River. *Water Resources Research* 53, no. 8: 6562–6578.
- Zhang, N., H.M. He, S.F. Zhang, X.H. Jiang, Z.Q. Xia, and F. Huang. 2012. Influence of reservoir operation in the upper reaches of the Yangtze River (China) on the inflow and outflow regime of the TGR-based on the improved SWAT model. *Water Resources Management* 26, no. 3: 691–705.

REBUILT. FROM THE GROUND UP.



VISIT THE NEW WELLOWNER.ORG TODAY!

WellOwner.org is supported by the Rural Community Assistance Partnership (RCAP.org), as part of the USEPA funded program "Improving Water Quality through Training and Technical Assistance to Private Well Owners."

 WellOwner.org

